www.ietdl.org

Published in IET Circuits, Devices & Systems
Received on 12th June 2010
Revised on 4th October 2010
doi: 10.1049/iet-cds.2010.0201

ISSN 1751-858X

All possible second-order four-impedance two-stage Colpitts oscillators

A.S. Elwakil M.A. Al-Radhawi

Department of Electrical and Computer Engineering, University of Sharjah, P.O. Box 27272, United Arab Emirates
E-mail: elwakil@ieee.org

Abstract: The authors report all the possible four-impedance settings that yield a valid second-order two-stage Colpitts oscillator. These settings are obtained following an exhaustive search conducted on two possible structures of the oscillator modelled through two-port network transmission parameters. Only valid second-order cases with a maximum of three reactive elements are reported. Experimental and Spice verification of a selected example using both MOS and BJT transistors is given.

1 Introduction

The two-stage Colpitts oscillator was reported in [1, 2] where it was used for ultra-high-frequency (UHF) waveform generation. Essentially, this two-stage Colpitts oscillator employs two transistors configured in a cascade topology, and hence inherits the high-frequency advantages of this well-known amplifier topology. Fig. 1 shows the structure of this oscillator as proposed in [1, 2] when BJT transistors are used. Four impedances are needed along side a biasing current source I_B and two biasing voltage sources V_{B1} and V_{B2}; one of these voltage sources is usually not necessary and can be substituted with a direct connection to ground. Corresponding to the structure in Fig. 1, the impedance setting that has been reported in [1, 2] assumed Z_1, Z_2 and Z_3 are capacitors of values C_1, C_2 and C_3, respectively, while Z_4 is an inductor L with internal resistance R in which case the ideal oscillation frequency was found to be

$$\omega_0 = \sqrt{\frac{C_1C_2 + C_2C_3 + C_1C_3}{LC_1C_2C_3} - \left(\frac{R}{L}\right)^2} \qquad (1)$$

What is not clear and has not been demonstrated is the following:

(i) Is this impedance setting necessary or can other settings be used? And what would be the oscillation start-up condition and oscillation frequency corresponding to each case?
(ii) Can the structure in Fig. 1 be realised using MOS transistors? Of course for UHF applications, the BJT has superior performance but it is still important to have an answer to this question particularly that a single-stage Colpitts oscillator can be well designed using an MOS transistor [3, 4].
(iii) Is the structure in Fig. 1 unique, not in terms of impedance settings but in terms of transistor terminal connections? More clearly, under AC conditions, the biasing voltage V_{B1} and V_{B2} are both ground connected. This implies that the two BJT transistors have their base terminals at common ground. However, there may be alternative valid structures where other terminals (e.g. the emitter terminals) are connected to the common ground, as was recently shown to be feasible for the one-transistor Colpitts oscillator in [5]. Accordingly, in [5] the single-stage Colpitts oscillator has been classified into three distinct classes (common-A, common-B and common-C) depending on the location of the common ground.

In this work, we use two-port network transmission parameters [5, 6] to model the two-stage Colpitts oscillator of Fig. 1. A general characteristic equation independent of whether the transistors used are BJT or MOS transistors is derived and a Matlab code is then written to symbolically find all possible impedance settings that would yield a valid oscillator under a set of constraints which subsequently narrows the search space. Having realised that the two-port network topology corresponding to Fig. 1 is a common-B/common-B topology, we investigate the remaining three possibilities and confirm that only one alternative topology; namely the common-B/common-A topology can yield a number of valid oscillators. Experimental and Spice simulation results are given for a selected design case.

2 Common-B/Common-B structure

The two-stage Colpitts oscillator of Fig. 1 is redrawn in two-port network form as shown in Fig. 2*a*. Each two-port network has three terminals labelled A, B and C which correspond to the emitter, base and collector of a BJT transistor (or the source, gate and drain of a MOS transistor). As such, it is clear from Fig. 2*a* that this structure is a common-B/common-B grounded structure. The two networks can be described by the transmission

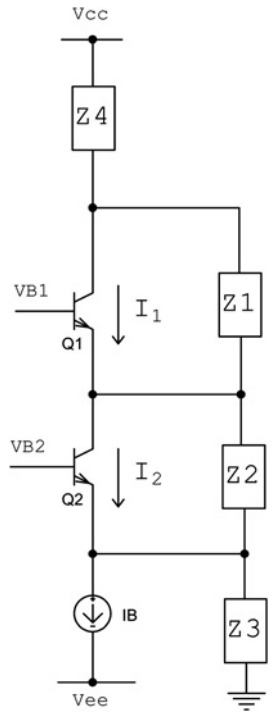

Fig. 1 *Two-stage Colpitts oscillator circuit*

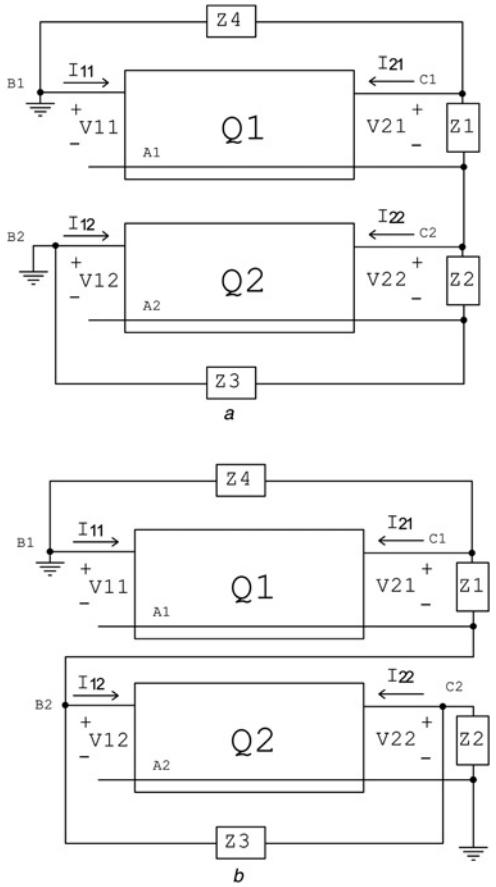

Fig. 2 *Two-port network representations of*

a Common-B/common-B two-stage Colpitts oscillators
b Common-B/common-A two-stage Colpitts oscillators

matrices [6]

$$\begin{pmatrix} V_{11} \\ I_{11} \end{pmatrix} = \begin{pmatrix} a_{11} & a_{12} \\ a_{21} & a_{22} \end{pmatrix} \begin{pmatrix} V_{21} \\ -I_{21} \end{pmatrix} \quad \text{and}$$
$$\begin{pmatrix} V_{12} \\ I_{12} \end{pmatrix} = \begin{pmatrix} b_{11} & b_{12} \\ b_{21} & b_{22} \end{pmatrix} \begin{pmatrix} V_{22} \\ -I_{22} \end{pmatrix} \tag{2}$$

where the terminal voltages (V_{11}, V_{12}, V_{21}, V_{22}) and the terminal currents (I_{11}, I_{12}, I_{21}, I_{22}) follow standard two-port notations (see Fig. 2*a*). It is possible to write the following KCL equations at nodes C_1, C_2 and A_2

$$I_{21} + \frac{V_{21}}{Z_1} + \frac{V_{21} - V_{11}}{Z_4} = 0; \quad I_{22} + \frac{V_{22}}{Z_2} - \frac{V_{21}}{Z_1} = 0$$
$$V_{22} - \frac{Z_2}{Z_3} V_{12} = 0 \tag{3}$$

which when used in conjunction with (2) while noting that $V_{11} = V_{12} - V_{22}$ enable the elimination of all variables and hence one obtains the general characteristic equation

$$\frac{a_{11}Z_4 + a_{12}(1 + Z_4/Z_1)}{a_{12} + Z_4} = -\frac{Z_2 + Z_3}{Z_1(1 + (b_{11}/b_{12})Z_2 + (1/b_{12})Z_3)} \tag{4}$$

Interestingly (4) is independent of a_{21}, a_{22}, b_{21} and b_{22}.

As derived in [5], the transmission matrix for an ideal BJT biased in the forward active mode and an ideal MOS transistor biased in the saturation mode are given respectively by

$$\begin{pmatrix} 0 & -\frac{1}{g_m} \\ 0 & -\frac{1}{\beta} \end{pmatrix}_{\text{BJT}} \quad \text{and} \quad \begin{pmatrix} 0 & -\frac{1}{g_m} \\ 0 & 0 \end{pmatrix}_{\text{MOS}} \tag{5}$$

where g_m is the small signal transconductance and β is the forward active current gain (Recall that for a BJT transistor in the forward active mode $g_m = I_C/V_T$ where I_C is the DC collector current and V_T is the thermal voltage ($\simeq$26 mV). For an MOS transistor in the saturation mode, $g_m = \sqrt{2kI_D}$ where I_D is the drain to source current and $k = \mu_{n,p}C_{ox}W/L$; $\mu_{n,p}$ is the electron or hole mobility, C_{ox} is the gate oxide capacitance and W/L is the aspect ratio). For $\beta \gg 1$, it is clear that both the ideal BJT and ideal MOS transistors are described by an identical transmission matrix where the only design parameter is g_m. This ideal matrix is the starting point for the design process whereas at a later stage, more sophisticated matrices, which take into consideration the parasitic effects can be used to evaluate the design performance in a robust and straightforward manner [5]. Assuming $\frac{1}{\beta} \to 0$ and substituting in (4) with the parameters

$$\begin{pmatrix} a_{11} & a_{12} \\ a_{21} & a_{22} \end{pmatrix} = \begin{pmatrix} 0 & -\frac{1}{g_{m1}} \\ 0 & 0 \end{pmatrix} \quad \text{and}$$
$$\begin{pmatrix} b_{11} & b_{12} \\ b_{21} & b_{22} \end{pmatrix} = \begin{pmatrix} 0 & -\frac{1}{g_{m2}} \\ 0 & 0 \end{pmatrix} \tag{6}$$

results in the simplified characteristic equation

$$\frac{Z_1 + Z_4}{Z_2 + Z_3} = \frac{1 - g_{m1} Z_4}{g_{m2} Z_3 - 1} \tag{7}$$

where g_{m1} and g_{m2} as the only design parameters.

A Matlab code was written in search for all possible oscillators that can be obtained from (7). To reduce the search space we have imposed the constraints that

1. the resulting characteristic equation will only be of second-order and
2. a maximum of three reactive elements (only one of which maybe an inductor) and two resistors are to be used in any valid circuit

After taking into consideration the DC biasing constraints (see Fig. 1), only nine valid cases were found and are summarised in Table 1 where the oscillation start-up condition (Hopf bifurcation condition) and the oscillation frequency expressions are both given for each case. It is of course well-known that the oscillation start-up condition obtained from linear analysis is necessary but insufficient as oscillators may actually latch-up and never oscillate [7]. However, the non-linear treatment of any oscillator configuration is to be done on an individual basis [8, 9]. Several observations are noted from Table 1; in particular:

1. Out of the nine cases that satisfy the constraints, five represent RC oscillators and four represent LC ones. The impedance setting reported in [1, 2] does not appear in the table since it yields a third-order characteristic equation and hence was eliminated from the Matlab search space. It may have been chosen in [1, 2] in order to produce chaos, which only appears in systems of order ≥ 3 [10].
2. There is only one truly second-order possible oscillator (case 6) since it employs two capacitors. The rest of the

Table 1 All possible cases for the common-B/common-B structure

	Z_1	Z_2	Z_3	Z_4	Start-up condition	$\omega_o^2 =$
1	C_1	C_2	$R_3 + L$	R_4	$\frac{g_{m1} + g_{m2}}{(R_3 + R_4)/R_3R_4} + \frac{g_{m2}}{C_1(R_3 + R_4)/L} = 1$ $g_m = \frac{R_3 + R_4}{2R_3R_4 + (L/C_1)}\Big\|_{g_{m1}=g_{m2}}$	$\frac{C_1(1 - g_{m1}R_4) + C_2(1 - g_{m2}R_3)}{C_1C_2L[1 - (g_{m1} + g_{m2})R_4]}$ $= \frac{1}{LC_{eff}} \frac{1 - (g_m(C_1R_4 + C_2R_3)/C_1 + C_2)}{1 - 2g_mR_4}\Big\|_{g_{m1}=g_{m2}}$
2			$R_3 \| C_3$		$\left(1 + \frac{C_3}{C_2}\right)g_{m1} + g_{m2} = \frac{R_3 + R_4}{R_3R_4} + \frac{C_1 + C_2}{C_1C_2}\frac{C_3}{R_4}$ $g_m = \frac{(R_3 + R_4/R_3R_4) + ((C_1 + C_2)/(C_1C_2))(C_3/R_4)}{2 + (C_3/C_2)}\Big\|_{g_{m1}=g_{m2}}$	$\frac{C_1(1 - g_{m1}R_4) + C_2(1 - g_{m2}R_3)}{C_1C_2C_3R_3R_4}$ $= \frac{1 - (g_m(C_1R_4 + C_2R_3)/C_1 + C_2)}{C_{eff}C_3R_3R_4}\Big\|_{g_{m1}=g_{m2}}$
3			$R_3 + C_3$		$\left(1 + \frac{C_3}{C_2}\right)g_{m1} + \left(1 + \frac{C_3R_3}{C_1R_4}\right)g_{m2} = \frac{1 + (C_3/C_2) + (C_3/C_1)}{R_4}$ $g_m = \frac{1 + (C_3/C_2) + (C_3/C_1)}{(2 + (C_3/C_2) + (C_3R_3/C_1R_4))R_4}\Big\|_{g_{m1}=g_{m2}}$	$\frac{g_{m2}}{C_1C_3[R_3R_4(g_{m1} + g_{m2}) - R_3 - R_4]} =$ $\frac{g_m/(2g_mR_{eff} - 1)}{C_1C_3(R_3 + R_4)}\Big\|_{g_{m1}=g_{m2}}$
4			R_3	$R_4 \| C_4$	$g_{m1} + \left(1 + \frac{C_4}{C_1}\right)g_{m2} = \frac{R_3 + R_4}{R_3R_4} + \frac{C_1 + C_2}{C_1C_2}\frac{C_4}{R_3}$ $g_m = \frac{(R_3 + R_4)/(R_3R_4) + ((C_1 + C_2)/(C_1C_2))(C_4/R_3)}{2 + (C_4/C_1)}\Big\|_{g_{m1}=g_{m2}}$	$\frac{C_1(1 - g_{m1}R_4) + C_2(1 - g_{m2}R_3)}{C_1C_2C_4R_3R_4} =$ $\frac{1 - (g_m(C_1R_4 + C_2R_3)/(C_1 + C_2)}{C_{eff}C_4R_3R_4}\Big\|_{g_{m1}=g_{m2}}$
5				$R + L$	$\left(1 + \frac{L}{C_2RR_3}\right)g_{m1} + g_{m2} = \frac{R_3 + R}{R_3R}$ $g_m = \frac{R_3 + R}{2RR_3 + (L/C_2)}\Big\|_{g_{m1}=g_{m2}}$	$\frac{C_1(1 - g_{m1}R) + C_2(1 - g_{m2}R_3)}{C_1C_2L[1 - (g_{m1} + g_{m2})R_3]} =$ $\frac{1}{LC_{eff}} \frac{1 - (g_m(C_1R + C_2R_3)/(C_1 + C_2))}{1 - 2g_mR_3}\Big\|_{g_{m1}=g_{m2}}$
6		R_2	C_3	R_4	$(g_{m1} + g_{m2})R_4 = 1 + \frac{C_1}{C_3}$	$\frac{g_{m2}}{C_1C_3[(g_{m1}R_4 - 1)R_2 - R_4]}$
7	$R + L$	C_2			$g_{m2} = \frac{C_3(R + R_4)}{L}$	$\frac{(C_2 + C_3)(1 - g_{m1}R_4) - g_{m2}(R_4 + R)C_2}{C_2C_3L}$
8	R_1			$R_4 \| C_4$	$g_{m2}R_1 = 1 + \frac{C_3}{C_2} + \left(1 + \frac{R_1}{R_4}\right)\frac{C_3}{C_4}$	$\frac{(1 - g_{m1}R_4)(1 + (C_3/C_2)) - g_{m2}(R_1 + R_4)}{C_3C_4R_1R_4}$
9				$R + L$	$\left(1 + \frac{C_3}{C_2}\right)g_{m1} + g_{m2} = \frac{R_1 + R}{L/C_3}$	$\frac{(1 - g_{m1}R)(C_2 + C_3) - g_{m2}(R_1 + R)C_2}{C_2C_3L}$

doi: 10.1049/iet-cds.2010.0201

cases are de-generating second-order systems which employ three reactive elements and under non-linear analysis will remain third-order. From the expression of ω_o corresponding to case 6, it is seen that it is necessary for the condition $1 + g_{m2}R_2 < C_1R_2/C_3R_4$ to hold.

3. In cases 2, 4 and 9, tuning of ω_o without affecting the start-up condition is not possible. Hence, these structures are not attractive. In the remaining cases, there is always one independent parameter which can be used for tuning. For example, in case 1 while ω_o depends on C_2 the start-up condition does not.

4. The first five cases in Table 1 have $Z_{1,2}$ as capacitors. With reference to Fig. 1, this implies that under DC conditions, the currents I_1 and I_2 are equal. For BJT transistors this automatically means that $g_{m1} = g_{m2}$. The same is true for MOS transistors if the two transistors have equal aspect ratios. The simplified expressions that are obtained in this case are given within Table 1 after defining $C_{eff} = C_1C_2/(C_1 + C_2)$ and $R_{eff} = R_3R_4/(R_3 + R_4)$. A design example of case 5 is given in Section 4.

5. Cases 7 and 8 are attractive since the start-up condition of both depends only on g_{m2} while ω_o depends on g_{m1}. This implies that electronic tuning of the oscillation frequency can be achieved through g_{m1}.

3 Common-B/Common-A structure

A novel alternative two-port network structure is shown in Fig. 2*b*. The structure represents a common-B/common-A structure because of the location of the common ground of the two transistors. It is possible to write the following KCL equations at nodes C_1, B_2 and C_2

$$I_{21} + \frac{V_{21}}{Z_1} + \frac{V_{21} - V_{11}}{Z_4} = 0; \quad I_{12} + \frac{V_{12} - V_{22}}{Z_3} - \frac{V_{21}}{Z_1} = 0$$
$$\frac{V_{22}}{Z_2} + \frac{V_{22} - V_{12}}{Z_3} + I_{22} = 0 \tag{8}$$

which when used with (2) and noting that $V_{12} = -V_{11}$ yield the general characteristic equation

$$\left(1 + \frac{Z_1}{Z_4} + \frac{a_{11}}{a_{12}}Z_1\right)\left(\frac{1}{Z_3} + \frac{b_{22}}{b_{12}} + \frac{(b_{21} - (b_{11}b_{22}/b_{12}) - (1/Z_3))(Z_3 + b_{12})}{b_{12}(1 + (Z_3/Z_2)) + b_{11}Z_3}\right) = -\frac{1}{a_{12}} + \frac{1}{Z_4} \tag{9}$$

which is independent of a_{21}, a_{22} but depends on all four parameters $b_{11} \to b_{22}$ of transistor Q_2; that is the one connected in a common-A configuration. Substituting with (6) in (9) yields the simplified characteristic equation

$$\frac{Z_1 + Z_4}{Z_2 + Z_3} = \frac{1 - g_{m1}Z_4}{1 + g_{m2}Z_2} \tag{10}$$

that is valid for ideal MOS and BJT transistors. Notice that (10) is different from (7).

A Matlab code was written to obtain all valid oscillators using (10) while maintaining the same constraints mentioned above. Taking into consideration the DC biasing requirements, only three possible circuits were found and are given in Table 2. It is noted from Table 2 that there are two LC and only one RC oscillators and that all structures are de-generating second-order systems. In addition, the

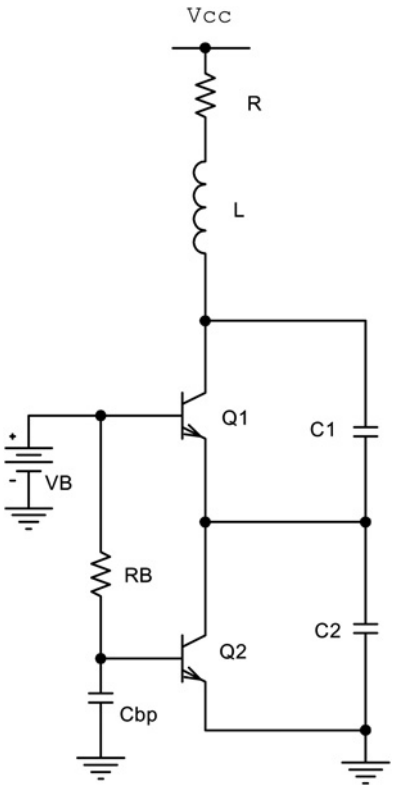

Fig. 3 *Implemented oscillator corresponding to case 5 of Table 1 with $Z_3 = R_3 = 0$*

Table 2 All possible cases for the common-B/common-A structure

	Z_1	Z_2	Z_3	Z_4	Start-up condition	$\omega_o^2 =$
1	C_1	$R + L$	C_3	R_4	$g_{m2}\left(1 + \frac{L}{C_1RR_4}\right) - g_{m1} = \frac{R + R_4}{RR_4}$	$\frac{C_1[g_{m2}(R_4 + (L/C_1R)) + (R_4/R)] - C_3(1 + g_{m2}R)}{LC_1C_3[g_{m2}(2R_4 + (L/C_1R)) + (R_4/R)]}$
2		R_2		$R + L$	$g_{m1}\left(1 + \frac{L}{C_3RR_2}\right) - g_{m2} = \frac{R + R_2}{RR_2}$	$\frac{C_1(1 - g_{m1}R) - C_3(1 + g_{m2}R_2)}{LC_1C_3[1 - (g_{m1} + g_{m2})R_2]}$
3				$R_4 \| C_4$	$g_{m1} - g_{m2}\left(1 + \frac{C_4}{C_1}\right) = \frac{R_2 + R_4}{R_2R_4} + \frac{C_4}{C_1R_2}$	$\frac{C_1(1 - g_{m1}R_4) - C_3(1 + g_{m2}R_2)}{C_1C_3C_4R_2R_4}$

start-up condition and oscillation frequency can be independently tuned in all cases.

We have also investigated the remaining two-stage Colpitts structures; that is, the common-A/common-A and the common-A/common-B topologies and found that both of them cannot yield any valid oscillators.

4 Design example

We choose to demonstrate a design example representing case 5 in Table 1. Recalling the design equations in the table and selecting $R_3 = 0$ and $C_1 = C_2 = C$, results in the start-up condition $g_m = RC/L$ and the oscillation frequency $\omega_o = \sqrt{((2 - g_m R)/LC)} = \sqrt{(2/LC) - (R/L)^2}$. Selecting $R = 1\,\text{k}\Omega$, $L = 1\,\text{mH}$ and $C = 100\,\text{pF}$ implies a start-up $g_m = 0.1\,\text{mA/V}$ with $f_o \simeq 693\,\text{kHz}$. Fig. 3 shows the implemented circuit using BJT transistors including the DC biasing circuitry composed of V_B, R_B and the bypass capacitor C_{bp}. Two BC107 transistors and a power supply $V_{cc} = 5\,\text{V}$ were used. C_{bp} was set equal to $10\,\mu\text{F}$, R_B was fixed as $1\,\text{M}\Omega$ and V_B was kept variable. At $V_B = 0.65\,\text{V}$, oscillations started with a measured oscillation frequency of $f_m = 600.9\,\text{KHz}$ and a measured DC collector current of $15\,\mu\text{A}$ which corresponds to $g_m \simeq 0.58\,\text{mA/V}$ slightly higher than the theoretical start-up value. The measured waveform across C_2 is shown in Fig. 4*a*. As V_B was increased, so did the amplitude of the sinusoid, as shown in Fig. 4*b* for $V_B = 0.75\,\text{V}$ ($g_m \simeq 1.7\,\text{mA/V}$), with a slight improvement in the oscillation frequency ($f_m = 609\,\text{kHz}$) towards its theoretical value. Oscillations could still be observed up till $V_B \simeq 2\,\text{V}$.

Note that our design choice of $R_3 = 0$ effectively implies that the oscillator of Fig. 3 is also a common-B/common-A oscillator; albeit with three impedances instead of four as compared to the structure in Fig. 2*b*. This means that the bypass capacitor C_{bp} may well be removed from the circuit. We have verified this option and the observed waveform in this case at $V_B = 0.75\,\text{V}$ is shown in Fig. 4*c* where $f_m = 669.5\,\text{kHz}$ is much closer to the theoretical value. The corresponding power spectrum is given in Fig. 4*d*. However, the maximum value of V_B until which oscillations were observed was approximately 1 V and the oscillation amplitude does not exceed $200\,\text{mV}_{p-p}$. Of course, only through non-linear modelling can the oscillation amplitude be accurately predicted [8, 9].

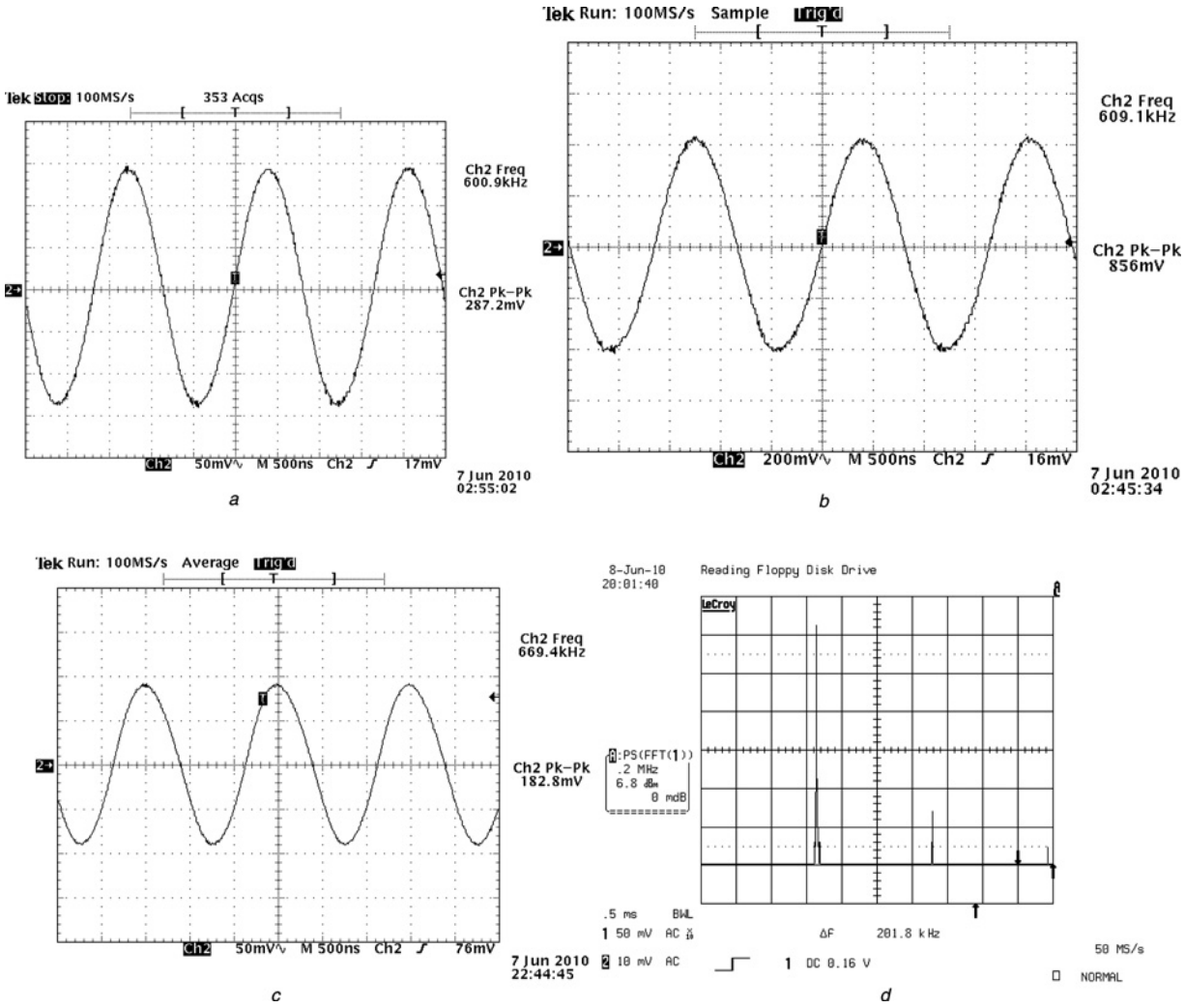

Fig. 4 *Experimental waveforms of the voltage across C_2 for the oscillator in Fig. 3 at*

a $V_B \simeq 0.65\,\text{V}$
b $V_B \simeq 0.75\,\text{V}$
c $V_B \simeq 0.75\,\text{V}$ with C_{bp} removed
d Corresponding power spectrum

doi: 10.1049/iet-cds.2010.0201

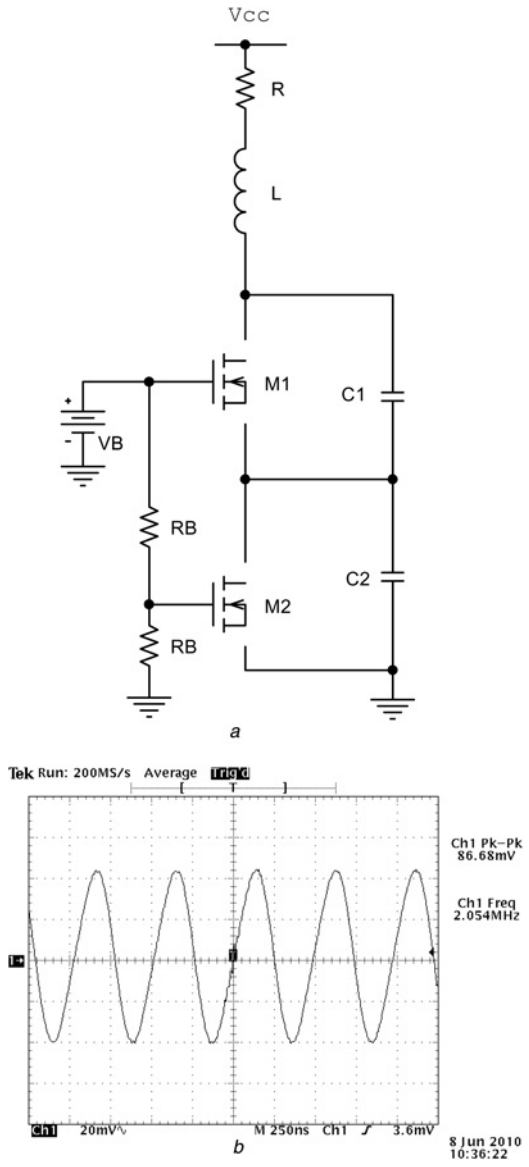

Fig. 5 *Design example of*

a MOS-based implementation of case 5 in Table 1 at $R_3 = 0$

b Observed waveform across C_2 ($L = 200\ \mu H$, $R = 120\ \Omega$)

Note that the biasing point was $V_{DS1} = 6.56\ V$, $V_{GS1} = 2.62\ V$, $V_{DS2} = V_{GS2} = 2.5\ V$

We have also verified the functionality of same structure using BS170 NMOS transistors, as shown in Fig. 5*a*. Owing to the high threshold voltage of this MOS transistor ($V_{TH} \simeq 2\ V$), a power supply $V_{cc} = 10\ V$ was used. Fixing $V_B = 5\ V$, $R_B = 10\ k\Omega$, $C_1 = C_2 = 100\ pF$ and $L = 200\ \mu H$ oscillations started at $R = 120\ \Omega$, corresponding to a bias current $I_{DS_{1,2}} = 25.5\ mA$. The observed waveform across C_2 is shown in Fig. 5*b*. It is of course evident that better performance can only be achieved on the integrated circuit

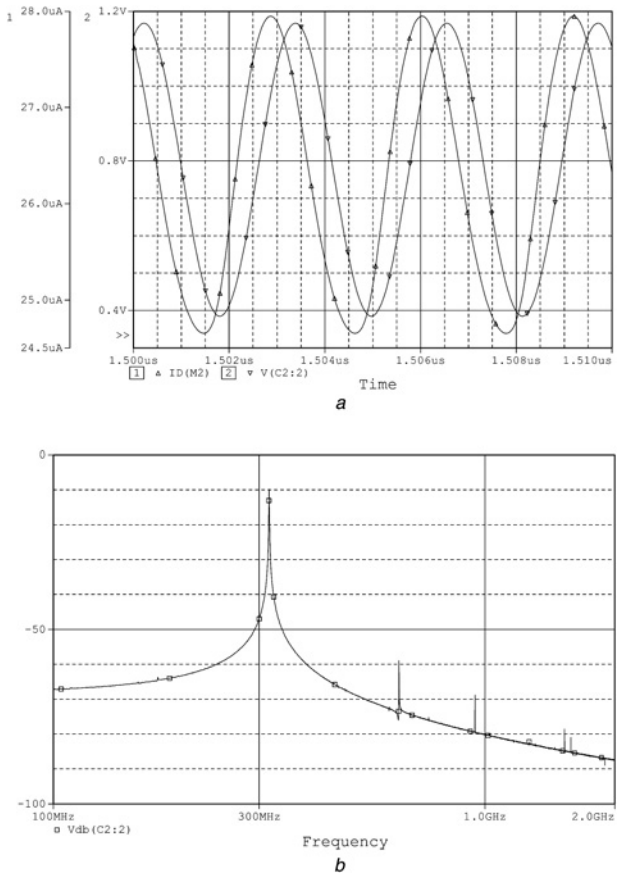

Fig. 6 *Spice simulation results for the oscillator in Fig. 5a using 0.25 μm CMOS parameters*

a Voltage across C_2 and current in M_2

b Corresponding spectrum

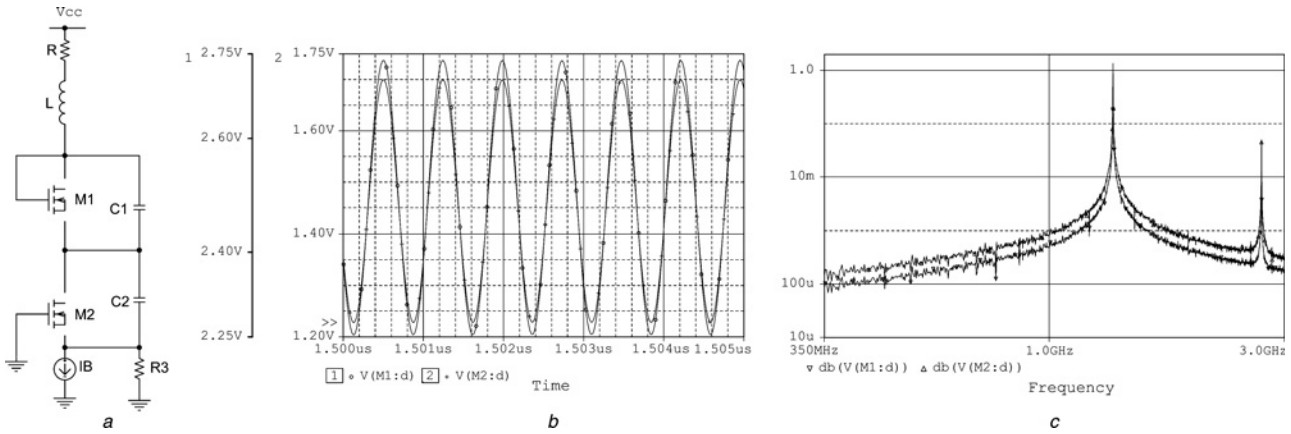

Fig. 7 *Oscillator designed to oscillate beyond the resonance frequency*

a Circuit structure

b Spice simulation results using 0.25 μm CMOS parameters at $I_B = 160\ \mu A$ of the voltage waveforms at the drains of M_1 and M_2, respectively

c Corresponding spectrum

level. The same oscillator shown in Fig. 5*a* was simulated in Spice using a BSIM 0.25 μm CMOS technology model with $V_{cc} = 2.5\,V$, $V_B = 1.5\,V$, $R_B = 10\,k\Omega$, $C_1 = C_2 = 1\,pF$ and $L = 0.5\,\mu H$. Here, R was fixed as $25\,\Omega$ and the transistor aspect ratios $(W/L)_{1,2}$ were used to start-up oscillations maintaining that $(W/L)_1 = (W/L)_2$. Fig. 6*a* shows the observed waveforms at $W/L = 2.5\,\mu m/1\,\mu m$. The corresponding DC current was $I_{DS_{1,2}} = 28.75\,\mu A$ and the power spectrum, shown in Fig. 6*b*, indicates an oscillation frequency of 316 MHz close enough to the theoretical value of 318.3 MHz with a measured THD of 1.95%.

Referring back to the expression of ω_o in Table 1-case 5, it can be seen that there is a possibility of extending the oscillation frequency beyond the resonance value given by $1/\sqrt{LC_{eff}}$. In particular, it is seen that $\omega_o^2 = (1/LC_{eff})((1 - 0.5g_m(R + R_3))/(1 - 2g_mR_3))$ for $C_1 = C_2$. Therefore by properly selecting g_mR_3 without changing the values of L, C_1 or C_2, the oscillation frequency can be made much higher. Fig. 7*a* shows a design example where R_3 is kept in the circuit, unlike the oscillator of Fig. 5*a*. Figs. 7*b* and *c* show the Spice simulation results for the same values corresponding to Fig. 6; that is, $C_1 = C_2 = 1\,pF$, $L = 0.5\,\mu H$, $R = 25\,\Omega$ and $V_{cc} = 2.5\,V$ while R_3 was selected as $100\,k\Omega$ and $(W/L)_{1,2} = 5\,\mu m/1\,\mu m$. Oscillations started at a bias current $I_B = 150\,\mu A$ and it is seen from Fig. 7*c* that the oscillation frequency is 1.347 GHz which is approximately four times higher than the resonance frequency of 318 MHz since $g_mR_3 \simeq 0.48$.

5 Conclusion

In this work we have derived the general characteristic equations for two classes of the two-stage Colpitts oscillator as a function of the two-port network transmission parameters. All different valid possibilities that yield a second-order oscillator with a maximum of three capacitors, or two capacitors and one inductor were found and a selected case was verified experimentally using discrete BJT and MOS transistors as well as by using a Spice BSIM 0.25 μm technology file. The Colpitts oscillator and its various derivatives continue to be significantly important circuit building blocks [11, 12].

6 References

1 Tamasevius, A., Mykolaitis, G., Bumeliene, S., *et al.*: 'Two-stage chaotic Colpitts oscillator', *Electron. Lett.*, 2001, **37**, pp. 549–551
2 Tamasevius, A., Bumeliene, G., Lindberg, E.: 'Improved chaotic Colpitts oscillator for ultrahigh frequencies', *Electron. Lett.*, 2004, **40**, pp. 1569–1570
3 Mayaram, K.: 'Output voltage analysis for the MOS Colpitts oscillator', *IEEE Trans. Circuits Syst. I*, 2000, **47**, pp. 260–263
4 Filanovsky, I., Verhoeven, C., Reja, M.: 'Remarks on analysis, design and amplitude stability of MOS Colpitts oscillator', *IEEE Trans. Circuits Syst. II*, 2007, **54**, pp. 800–804
5 Elwakil, A., Ahmed, W.: 'On the two-port network classification of Colpitts oscillators', *IET Circuits Devices Syst.*, 2009, **3**, pp. 223–232
6 Alexander, C., Sadiku, M.: 'Fundamentals of electric circuits' (McGraw-Hill, Singapore, 2007)
7 Elwakil, A.: 'On the necessary and sufficient conditions for latch-up in sinusoidal oscillators', *Int. J. Electron.*, 2002, **89**, pp. 197–206
8 Maggio, G., De feo, O., Kennedy, M.: 'Nonlinear analysis of the Colpitts oscillator and applications to design', *IEEE Trans. Circuits Syst. I*, 1999, **46**, pp. 1118–1130
9 Elwakil, A., Salama, K.: 'Higher-dimensional models of cross-coupled oscillators and application to design', *J. Circuits Syst. Comput.*, 2010, **19**, pp. 787–799
10 Kennedy, M.: 'Three steps to chaos – Part-I: evolution', *IEEE Trans. Circuits Syst. I*, 1993, **40**, pp. 640–656
11 Yodprasit, U., Enz, C., Gimmel, P.: 'Common-mode oscillation in capacitive coupled differential Colpitts oscillators', *Electron. Lett.*, 2007, **43**, pp. 1127–1128
12 Chen, Y., Mouthaan, K., Ooi, B.: 'Performance enhancement of Colpitts oscillators by parasitic cancellation', *IEEE Trans. Circuits Syst. II*, 2008, **55**, pp. 1114–1118

doi: 10.1049/iet-cds.2010.0201